

Supplemental Data

A Mitochondria-K⁺ Channel Axis Is Suppressed

in Cancer and Its Normalization

Promotes Apoptosis and Inhibits Cancer Growth

Sébastien Bonnet, Stephen L. Archer, Joan Allalunis-Turner, Alois Haromy, Christian Beaulieu, Richard Thompson, Christopher T. Lee, Gary D. Lopaschuk, Lakshmi Puttagunta, Sandra Bonnet, Gwyneth Harry, Kyoko Hashimoto, Christopher J. Porter, Miguel A. Andrade, Bernard Thebaud, and Evangelos D. Michelakis

Supplemental Results

DNA Microarrays Reveal a Short List of DCA-Regulated Genes Related to Mitochondria, Apoptosis and Ion Channels

We used DNA microarrays to profile the effects of DCA on gene expression in both A549 and M059K cell lines. We used a “subtraction” strategy to reveal relevant changes in tumor gene expression (at least 1.5 fold change) that were both due to DCA and evident in both tumors, rather than reflecting idiosyncratic tumor-specific gene changes. This gave us a list of 357 genes (NCBI, <http://www.ncbi.nlm.nih.gov/projects/geo/>), on which pathway analysis revealed genes related to mitochondria, apoptosis and ion channels (Supplement Figure 6). This short list of genes, included several ETC-I-related and many apoptosis-cell-cycle related genes, which mostly favor mitochondria-dependent apoptosis. All Kv channels in this list were upregulated and the biggest increase was in the Shaker Kv family, which includes Kv1.5 (KCNA5). This relatively non-constrained genomic survey confirmed our hypothesis-driven findings that DCA primarily enhances mitochondrial function and secondarily upregulates Kv1.5 expression, thereby enhancing apoptosis.

Supplemental Experimental Procedures

Cell Cultures: The cancer cell lines were purchased from ATCC (Manassas, VA). Healthy human small airway epithelial cell (SAEC, #CC-0294) were purchased from Cambrex BioScience (Guelph, Ontario). Healthy human fibroblasts were purchased from ATCC (#CCL-212). Healthy pulmonary artery smooth muscle cells (PASMC) were derived from the lungs of a lung transplant donor. The

A549 cells were maintained on F12K medium, glioblastoma on DMEM/F12, (Gibco/Invitrogen, Ontario), MCF-7 cells on DMEM (Sigma-Aldrich, Ontario); SAEC and fibroblasts on manufacturer's medium and PASMOC in DMEM. All media were supplemented with 10% FBS and 5% PSF (Gibco) as antibiotic. Dichloroacetate (0.05, 0.5, 5 mM, Sigma, St Louis), t-butyryl-H₂O₂ (100 μM) (Sigma) or VIVIT 4μM (a competitive peptide inhibitor of NFAT, "MAGPHPVIVITGPHEE", Calbiochem, San Diego, CA) were prepared as an aqueous solution and added to the medium of confluent cells. Cultures were incubated for up to 48h prior to harvesting.

Confocal Microscopy: Imaging was performed using a Zeiss LSM 510 confocal microscope and multiple-staining techniques as previously described (McMurtry et al., 2005; McMurtry et al., 2004). Apoptag apoptosis detection kit (TUNEL stain, Serologicals, Norcross, GA) and the proliferating cell nuclear antigen (PCNA) antibody (DAKO, Carpinteria, CA) were used as previously described (McMurtry et al., 2005; McMurtry et al., 2004). Nuclear staining was performed with 4',6'-diamidino-2-phenylindole dihydrochloride (DAPI, 300nM; Molecular Probes) in fixed tissues or cells as previously described (McMurtry et al., 2005). Apoalert Annexin V kit (Clontech, Palo Alto, CA), antibodies to cytochrome c (1:100 dilution, Calbiochem), apoptosis inducing factor (1:100 dilution, Santa Cruz, CA), NFAT-1 (1:100 dilution, cat#ab2722 Novus Biological), Kv1.5 (1:100 dilution, Sigma), survivin (1:100, Novus Biological) as well as mitotracker red (500 nM, Molecular Probes) were used as previously described (McMurtry et al., 2005; McMurtry et al., 2004). Mitochondrial membrane potential ($\Delta\Psi_m$) was studied in live cells (McMurtry et al., 2005; McMurtry et al., 2004), using tetramethyl-rhodamine methyl-ester perchlorate (TMRM) (10 nmol/L, x30 minutes, 37°C) and Hoechst (0.5μmol/L nuclear staining x10 minutes), both from Molecular Probes, Eugene, OR. Mitochondrial superoxide production was measured using Mitosox™(5μM Molecular Probes, Eugene OR), a cell-permeable ethidium bromide-derivative that is selectively targeted to the mitochondria, where it is oxidized by superoxide creating red fluorescence (excitation/emission 510/580nm).

Metabolic Studies: A549 cells were grown to confluency in T-175 flasks and rates of glycolysis (GI), fatty acid oxidation (FAO), and glucose oxidation (GO) were measured as previously described (Saddik et al., 1993) in the presence or absence of DCA (0.5mM, x48hr). To measure GI rates, cells were incubated in Krebs'-Henseleit buffer supplemented with 1.2 mM palmitate and 5 mM [5-³H]-glucose and assessed for ³H₂O. For FAO, the Krebs'-Henseleit solution contained 1.2 mM [9,10-³H]-palmitate and 5 mM glucose and assessed for ³H₂O. For GO, the buffer contained 1.2 mM palmitate and 5 mM [U-¹⁴C]-glucose and assessed for ¹⁴CO₂ production. Rates of energy metabolism were found to be linear to 360 minutes and therefore metabolic rates were determined over a 180 min period.

Immunoblotting: Cells or tumors were collected and immunoblotting was performed on pooled samples from 4 T-25 dishes or 4 rats/group (25 µg protein in pooled sample/lane). The films were digitized and quantified using 1D Image Analysis Software (Kodak, Rochester, NY). Expression was normalized to Ponceau-S to correct for loading differences as previously described (McMurtry et al., 2005; McMurtry et al., 2004). Antibodies: Kv1.5 (1:500, Sigma, Oakville, Ontario), survivin (1:1000, Novus Biologicals, Littleton, CO), caspase 3 (1:500, Upstate, Charlottesville, VA), caspase 9 (1:1000, Upstate), human PDK2 (1:200, Santa Cruz Biotechnologies, Santa Cruz, CA).

Quantative RT-PCR (qRT-PCR): Samples were added to a microwell plate with TaqMan probes and RT-PCR reagents (Applied Biosystems, Foster City, CA). qRT-PCR was performed with an ABI PRISM 7700 Sequence Detector (Applied Biosystems) and primers for human Kv1.5, Kir2.1, survivin, PDK2 and 18s as previously described (McMurtry et al., 2005; McMurtry et al., 2004).

Intracellular pH Measurement: the carboxy-seminaphthorhodafluor-1 (Snarf-1) was used to measure intracellular pH. Cells were loaded with 5 µM Snarf-1/AM for 45 min at 37° degrees in DMEM solution. Fluorescence was measured with confocal microscopy simultaneously at 640 nm (the unprotonated form) and 587 nm (protonated form); the ratio 640 nm/587 nm was used to visualize a change in intracellular pH.

Lactate Measurements: Extracellular lactate levels were measured spectrophotometrically using a SYNCHRON LX and Beckman coulter LX20 (Fullerton, CA USA) system at the clinical laboratory of the University of Alberta Hospital. Lactate was measured in the extracellular fluid of A549 cells incubated with and without DCA; measurements were made immediately and during the transfer to the clinical laboratory the specimens were kept on ice.

Intracellular K⁺: Cells were loaded in PPS (in mM:141 NaCl, 4.7 KCl, 1.8 CaCl₂, 1.2 MgCl₂, 10 HEPES, and 10 glucose pH7.4 with 5M NaOH) containing the acetoxymethyl ester form of PBFI (PBFI-AM; 5µM, Molecular Probes) for 40 min at 37°C. The PBFI-loaded cells were superfused with PPS for 30 min at room temperature to wash away extracellular dye and permit intracellular esterases to cleave cytosolic PBFI-AM into PBFI. PBFI fluorescence, which increases with increasing K⁺ concentration, was measured ratiometrically with a PTI *Delta scan 1* fluorescence spectrophotometer (PTI, London, ON, Canada) using an excitation ratio technique [excitation wavelength=340/380nm, emission wavelength=500nm] in which the signal at 340 nm corresponds to the maximal sensitivity of the probe to K⁺ and the signal at 380 nm corresponds to the isosbestic point of the probe.

Magnetic Resonance Imaging (MRI): Rat MRI was performed on a 1.5T Siemens Sonata MRI scanner with a 3 cm diameter surface radiofrequency coil centered over the tumor site. Thirty 1.5 mm

thick (no inter-slice gap) axial, T2-weighted images were acquired with and without fat saturation using the following parameters: repetition time (TR)=3710 ms, spin echo time (TE)=117 ms, 4 averages, field-of-view 90x90 mm, 256x256 matrix. This yielded an in-plane resolution of 0.35 mm x 0.35 mm and a voxel resolution of 0.185 mm³ in an acquisition time of 4.2 min.

DNA Microarrays: Total RNA from A549 and MO59K cells untreated and treated with DCA (0.5 mM for 48hrs) was extracted using Quiagen RNeasy kit (Ontario, Canada). Differences in gene expression among the 4 groups were assessed using human DNA chip set U133A (Affymetrix, California, USA). Analysis was performed using Affymetrix software. Where a gene was represented by multiple probe sets on the microarray, one probe set was chosen to represent the gene; when possible we chose a probe set specific for the gene, rather than one known to detect multiple genes. Probe sets whose hybridization was either increased or decreased by DCA both in A549 and M059K were selected (with at least one of those changes being significant according to a threshold of p-value and a fold change equal or larger than 1.5). A total of 357 probes sets fulfilled this. Pathway analysis for genes related to mitochondrial-redox function, apoptosis/cell cycle and ion channels, resulted in the list of genes and the heat map shown in Figure 8. Red bars indicate higher levels of hybridization, green lower levels, relative to the median level for each probe set.

The data produced in the four DNA microarray experiments described in this manuscript has been deposited in the Gene Expression Omnibus repository of gene expression data (NCBI, <http://www.ncbi.nlm.nih.gov/projects/geo/>) and can be accessed as a series (database identifier GSE6014) or sample by sample (database identifiers GSM139658 for control lung carcinoma, GSM139662 for control glioblastoma cells, GSM139665 for DCA treated glioblastoma cells, and GSM139670 for DCA treated lung carcinoma cells).

Supplemental References

McMurtry, M. S., Archer, S. L., Altieri, D. C., Bonnet, S., Haromy, A., Harry, G., Bonnet, S., Puttagunta, L., and Michelakis, E. D. (2005). Gene therapy targeting survivin selectively induces pulmonary vascular apoptosis and reverses pulmonary arterial hypertension. *J Clin Invest* 115, 1479-1491.

McMurtry, M. S., Bonnet, S., Wu, X., Dyck, J. R., Haromy, A., Hashimoto, K., and Michelakis, E. D. (2004). Dichloroacetate prevents and reverses pulmonary hypertension by inducing pulmonary artery smooth muscle cell apoptosis. *Circ Res* 95, 830-840.

Saddik, M., Gamble, J., Witters, L. A., and Lopaschuk, G. D. (1993). Acetyl-CoA carboxylase regulation of fatty acid oxidation in the heart. *J Biol Chem* 268, 25836-25845.

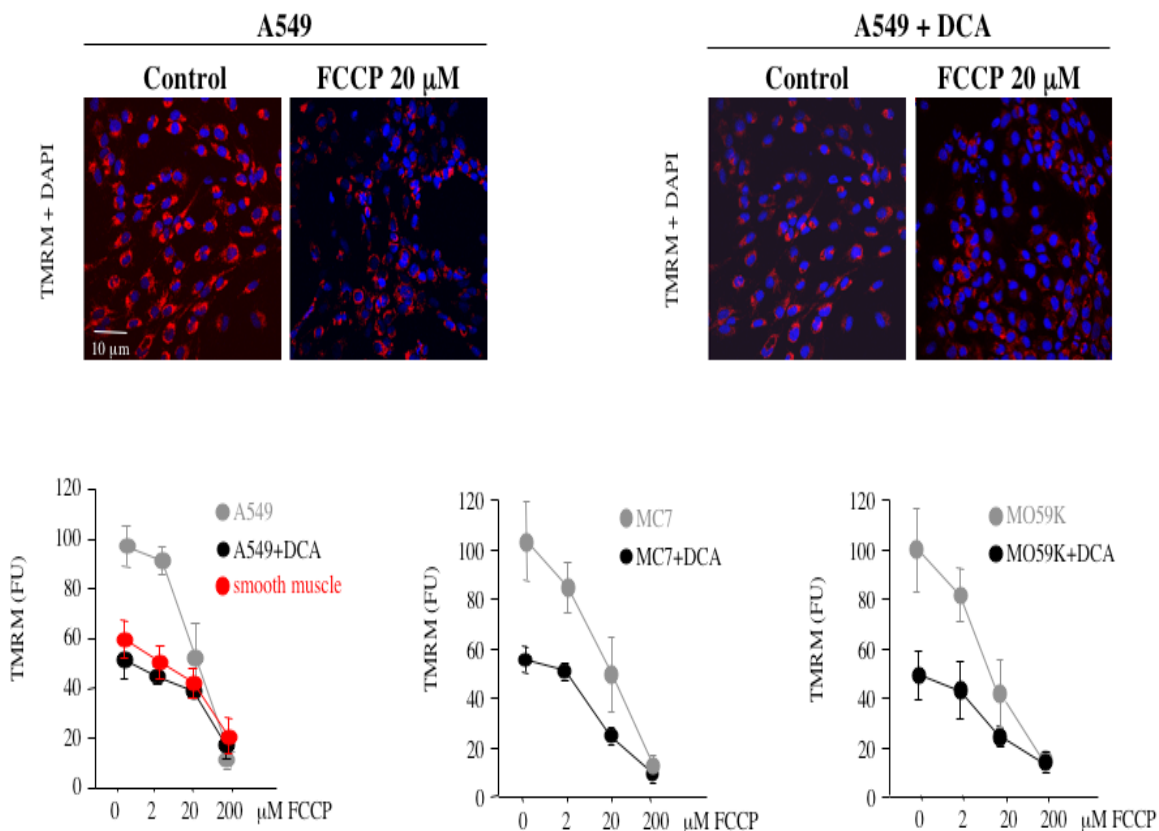


Figure S1. FCCP Depolarizes Untreated and DCA-Treated Cancer Cells to the Same Degree of $\Delta\Psi_m$

FCCP decreases $\Delta\Psi_m$ in a dose-dependent manner in both untreated and DCA-treated cancer cells (3 different cancer cell lines) and non-cancer cells (pulmonary artery smooth muscle cells, SMC).

Although the DCA-treated cells have a lower baseline $\Delta\Psi_m$, compared to the untreated cancer cells, they show a similar degree of depolarization in response to a protonophore, suggesting that their baseline differences in TMRM fluorescence are due to differences in $\Delta\Psi_m$ and not confounded by differences in the plasma membrane potential (E_m). n~15 plates (~190 cells)/group.

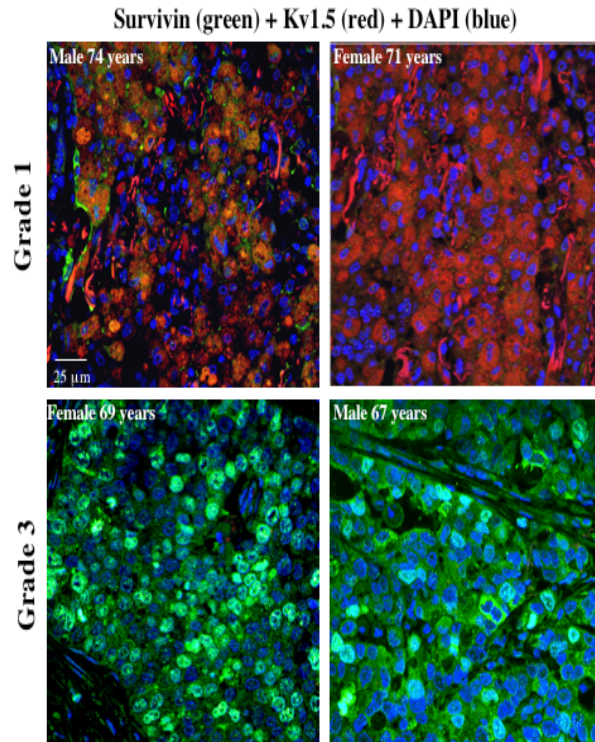
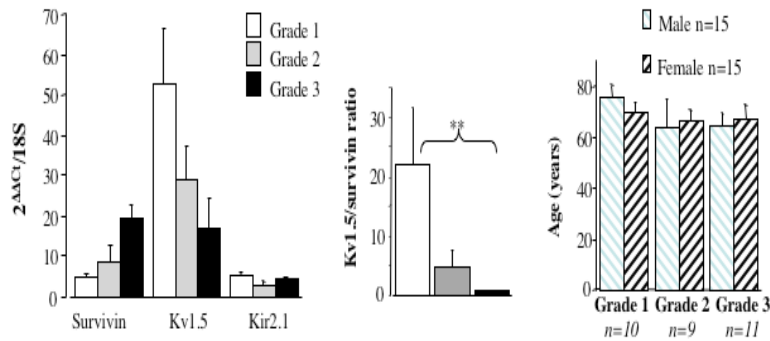


Figure S2. Human Non-Small Cell Lung Tumor Histology Grade Correlates Negatively with Kv1.5 and Positively with Survivin

A: qRT-PCR in archived tumors from 30 patients reveals that the higher the tumor grade (i.e. the more aggressive the tumor) the less the Kv1.5 and the more the survivin. Because both survivin and Kv1.5 mRNA were measured in each patient, we were able to create a “Kv1.5/survivin” index, which correlated even better with tumor grade. The tumors were graded in a blinded manner and the differences among the 3 histological grade groups were not because of differences in the age or sex of the patients. (n=30, **p<0.05).

B: Immunohistochemistry confirmed our qRT-PCR data as grade 1 tumors have less survivin (green) and more Kv1.5 (red) and the opposite is true for grade 3 tumors.

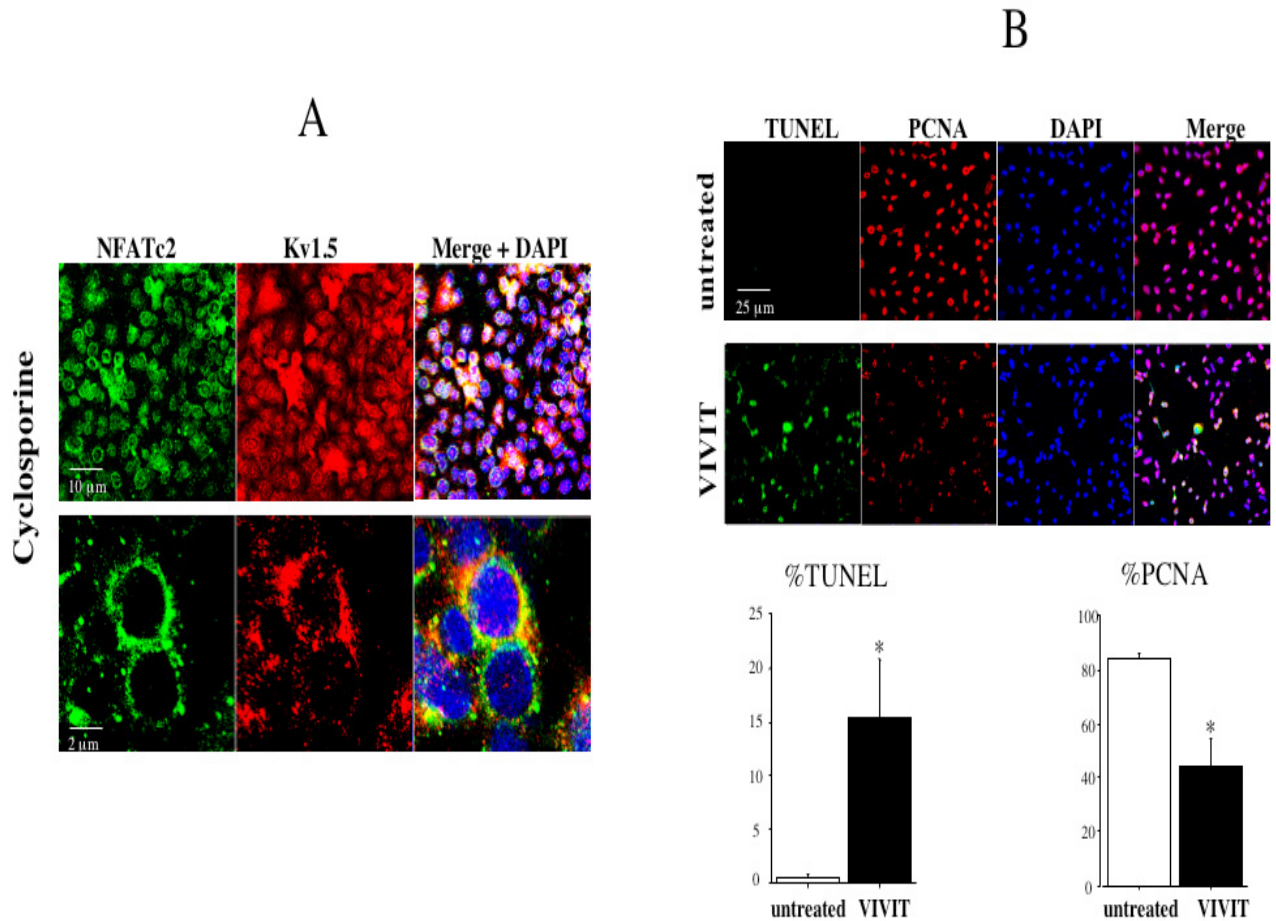


Figure S3. NFAT Inhibitors Mimic the Effects of DCA on Kv1.5 Expression and Apoptosis/Proliferation

A: Incubation of A549 cells with Cyclosporine 10 μ g/ml (a nonspecific inhibitor of calcineurin), inhibits NFAT1 (removed from the nucleus) and mimics DCA by upregulating Kv1.5 expression (for the untreated cells see Figure B).

B: The specific NFAT inhibitor VIVIT (which displaces NFAT1 from the nucleus, upregulates Kv1.5 and decreases intracellular Ca⁺⁺, see Figure 5C,D) increases apoptosis (%TUNEL-positive cells) and decreases proliferation (%PCNA-positive cells) in A549 cells (n~20 plates/group)

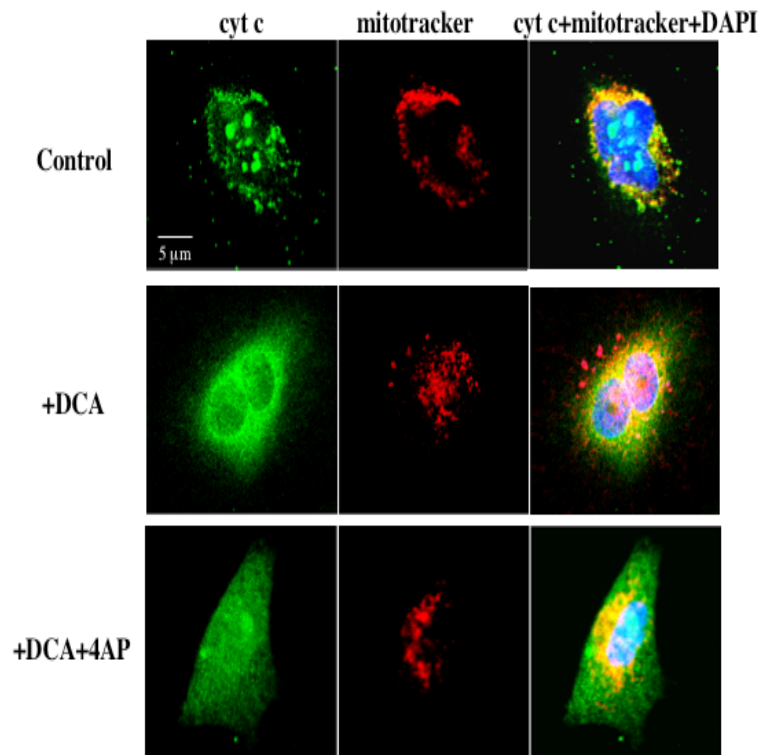
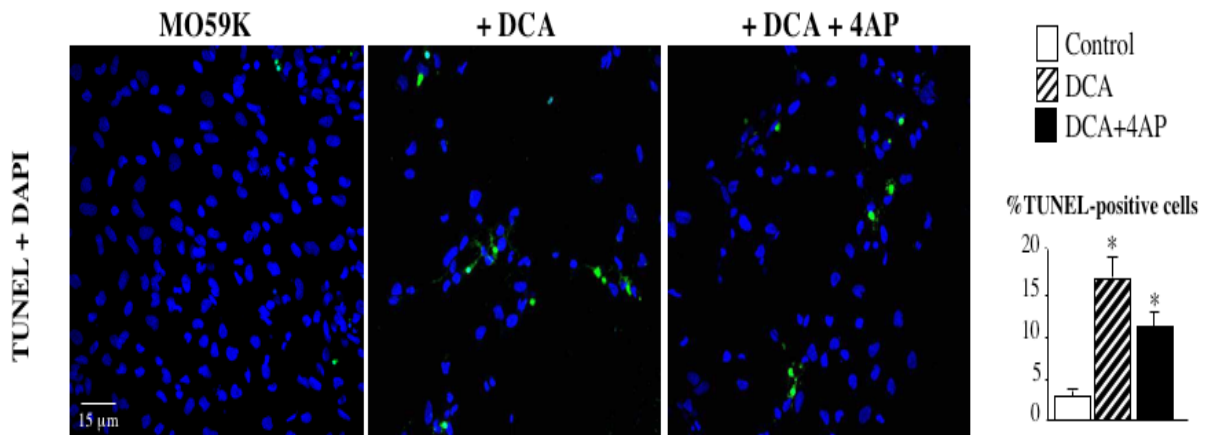


Figure S4. Kv Channel Inhibition Decreases DCA-Induced Apoptosis in Glioblastoma Cells by ~38% and Does Not Affect Efflux of Cytochrome c From Mitochondria.

Top: The Kv channel blocker 4-aminopyridine (5mM, 48 hrs) decreases by 38% the DCA induced apoptosis (% TUNEL positive cells) in glioblastoma cells (compared to 32% in A549 cells – see Figure 6D).

Bottom: The presence of 4-aminopyridine does not prevent the DCA-induced efflux of cytochrome c (green) from mitochondria (mitotracker red), as shown by the diffuse pattern of the cytochrome c staining (compared to the co-localization with the mitochondria in the untreated control cells)

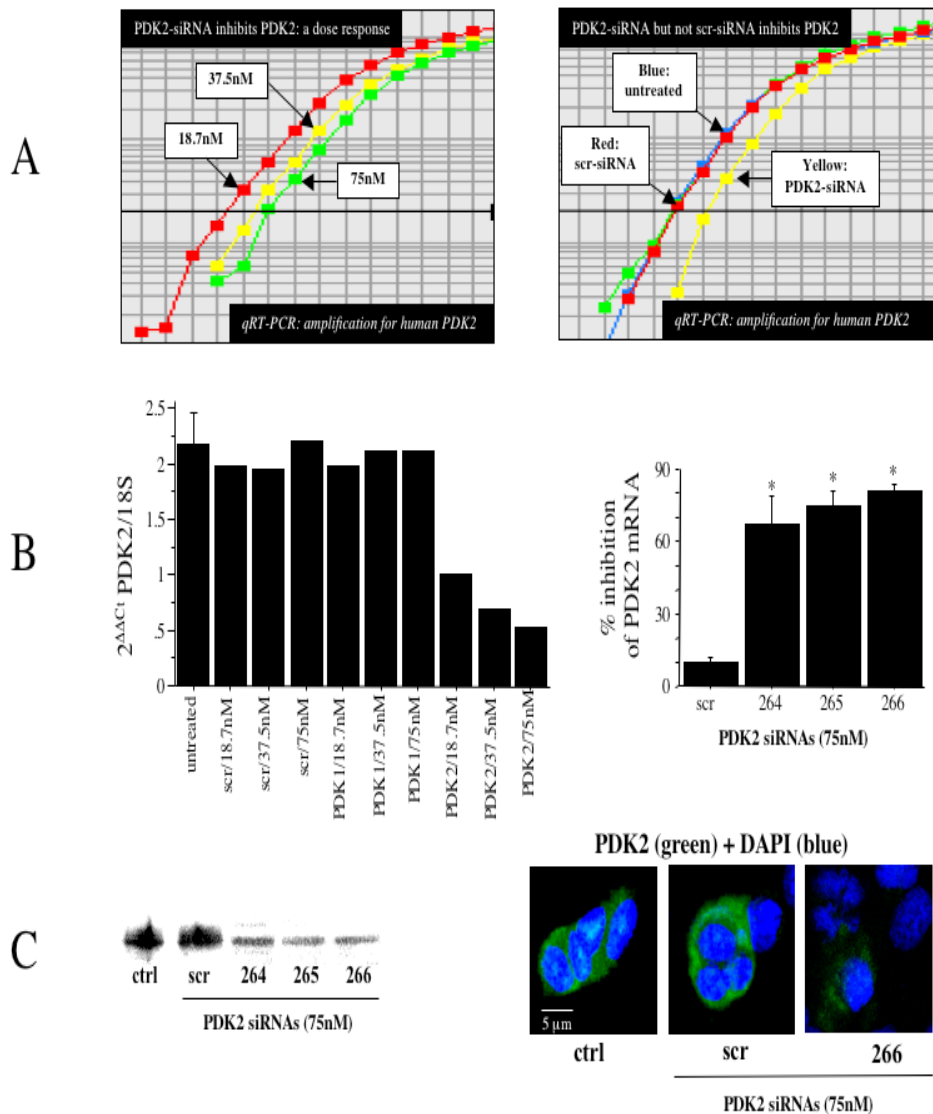


Figure S5. Effective and Selective Molecular Inhibition of PDK2 in A549 Cells Using siRNA

A: Representative amplification curves of human PDK2 mRNA levels in response to treatment with increasing doses of PDK2-siRNA (left) versus scrambled siRNA (right). The X axis is cycle numbers; the lower the mRNA levels the more the shift to the right.

B: Left: Increasing doses of scrambled siRNA and siRNA against human PDK1 do not decrease PDK2 expression. In contrast, siRNA against PDK2 (#266), inhibits gene expression in a dose-dependent manner. **Right:** Three different commercially available siRNAs for human PDK2 inhibit PDK2 expression in a similar manner. #266 was used for the experiments shown in Figure 7.

n=5, p<0.001 compared to the effects of the scrambled siRNA.

C: siRNA for PDK2 (but not scrambled siRNA) significantly inhibit PDK2 protein expression in A549 cells (immunoblot left, immunocytochemistry right).

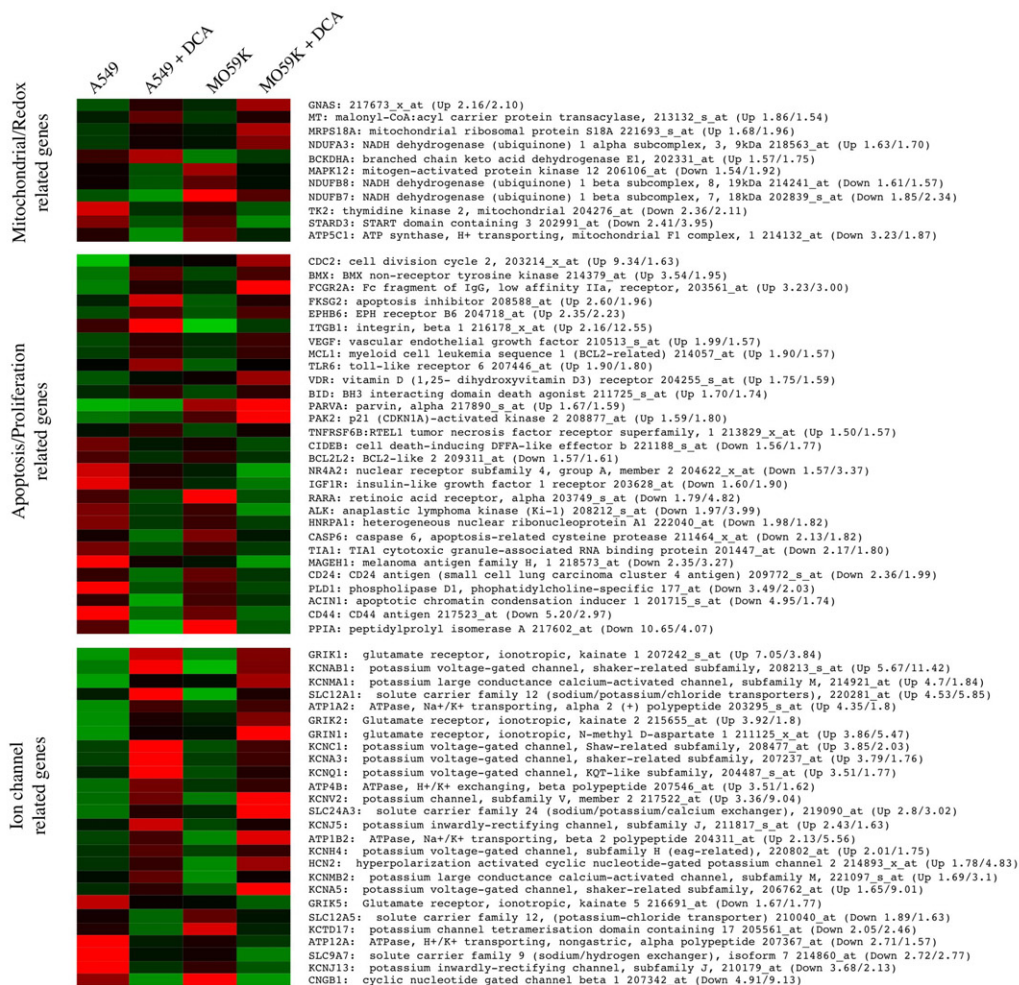


Figure S6. DCA Modulates Mitochondrial, Apoptosis/Proliferation and Ion Channel Genes

DNA microarrays analysis of both A-549 (DCA-treated and untreated) and MO59K (DCA-treated and untreated) showed that DCA modulates mitochondrial, apoptosis and ion channels related genes. The heat map lists genes corresponding to probe sets whose hybridization values were altered by DCA (by at least 1.5 fold) in both the A549 and MO59K cells (see methods). Red bars indicate higher levels of hybridization and green lower levels, relative to the median level for each probe set.